Improved Experimental Determinations of Phase Equilibria and Structural Transitions of Mixed Gas Hydrates under Isothermal Conditions

ARTICLE *in* ENERGY & FUELS · SEPTEMBER 2013

Impact Factor: 2.79 · DOI: 10.1021/ef401072s

8 AUTHORS, INCLUDING:

Minchul Kwon
Korea Advanced Institute of Science and Tech…
7 PUBLICATIONS **16** CITATIONS
SEE PROFILE

Yongwon Seo
Ulsan National Institute of Science and Techn…
55 PUBLICATIONS **1,062** CITATIONS
SEE PROFILE

Jaehyoung Lee
Korean Institute of Geoscience and Mineral Re…
29 PUBLICATIONS **329** CITATIONS
SEE PROFILE

energy&fuels

Article

pubs.acs.org/EF

Improved Experimental Determinations of Phase Equilibria and Structural Transitions of Mixed Gas Hydrates under Isothermal Conditions

Minchul Kwon,[†] Yeobum Youn,[†] Yongwon Seo,[‡] Jong-Won Lee,[§] Jaehyoung Lee,[#] Joo Yong Lee,[#] Se-Joon Kim,[#] and Huen Lee*[,†,∥]

[†]Department of Chemical and Biomolecular Engineering, KAIST, 291 Daehak-ro, Yuseong-gu, Daejeon 305-701, Republic of Korea

[‡]School of Urban and Environmental Engineering, Ulsan National Institute of Science and Technology (UNIST), 50 UNIST-gil, Eonyang-eup, Ulju-gun, Ulsan 689-798, Republic of Korea

[§]Department of Environmental Engineering, Kongju National University, 275 Budae-dong, Cheonan, Chungnam 331-717, Republic of Korea

[#]Petroleum and Marine Resources Division, Korea Institute of Geoscience and Mineral Resources (KIGAM), 92 Gwahang-no, Yuseong-gu, Daejeon 305-350, Republic of Korea

[∥]Graduate School of EEWS (Energy, Environment, Water and Sustainability), KAIST, 291 Daehak-ro, Yuseong-gu, Daejeon 305-701, Republic of Korea

Supporting Information

ABSTRACT: Investigations on the intrinsic properties of gas hydrates with multiple guests are essential to scientific and technological fields. In particular, even though evaluating and designing a hydrate phase process require isothermal phase equilibria, it is difficult to obtain extensive data with various components and compositions in a short period of time due to the static-analytic method. The present study introduces a new experimental determination on hydrate phase equilibria using continuous dissociation induced by extremely slow vapor volume expansion at a constant temperature. When a syringe pump is automatically operated at the microliter level during the dissociation process, the endothermic dissociation can be traced from the temperature readings. The validity and stability of the proposed technique were evaluated using pure CH_4 hydrates, and repeated measurements of three-phase (L_W−H−V) equilibrium conditions are used to optimize the volumetric expansion rates. Then, an experimental approach is applied to incipient $CH_4 + C_2H_6$ hydrates and identifies the structural transition behavior. This method is thought to provide extensive data and further improvements in terms of hydrate phase equilibria with multiple gas components.

1. INTRODUCTION

Gas hydrates are nonstoichiometric inclusion compounds formed with hydrogen-bonded water frameworks and encaged gaseous species under specific conditions.[1] These solid systems (single or multiple gases + H_2O) can be characterized by their intrinsic properties including phase equilibria and crystal structures (structures I, II, and H).[1−4] The thermodynamic equilibria of gas hydrates with a single gas are strongly dependent on molecular size and formation conditions, that is, formation pressure (p) and temperature (T). In contrast, gas hydrates with two or more guest components exhibit complex phase equilibria because mixture compositions play a decisive role as an intensive quantity in addition to p and T.

Thermodynamic studies of mixed gas hydrates provide not only hydrate dissociation conditions for respective composition but also further insights into the distribution of guest molecules over several types of cavities. In particular, drastic changes in thermophysical parameters, such as cage occupancy, hydration number, and dissociation enthalpy, are involved during the solid−solid phase transitions between different types of hydrate structures.[4−6] Among a variety of applications for mixed gas hydrates, many researchers have focused on the flow assurance in the petroleum industry as well as on the exploitation of naturally occurring gas hydrates (NGH) in oceanic sediments and permafrost regions.[4−17] Thermophysical properties of NGH reflect the fact that the precise composition of light hydrocarbon mixtures differs on the basis of exploration and production sites.[18,19] These studies have recently been extended to include the separation and storage of certain gases from mixed streams,[20−22] for example, selective CO_2 capture.[23,24] In addition, the replacement of CH_4 from NGH with CO_2 or ($N_2 + CO_2$) mixtures is thought to be a promising means of NGH production, simultaneously offering the opportunity for geological sequestration of CO_2 into deep ocean.[25−30]

According to the Gibbs phase rule for nonreacting systems,[31] the number of degrees of freedom becomes equal to the number of guest species on the condition that three phases of water-rich liquid (L_W), incipient hydrate (H), and vapor (V) coexist in equilibrium with each other. In this general case, the

Received: June 7, 2013
Revised: August 21, 2013
Published: August 21, 2013

dx.doi.org/10.1021/ef401072s | Energy Fuels 2013, 27, 5144−5152

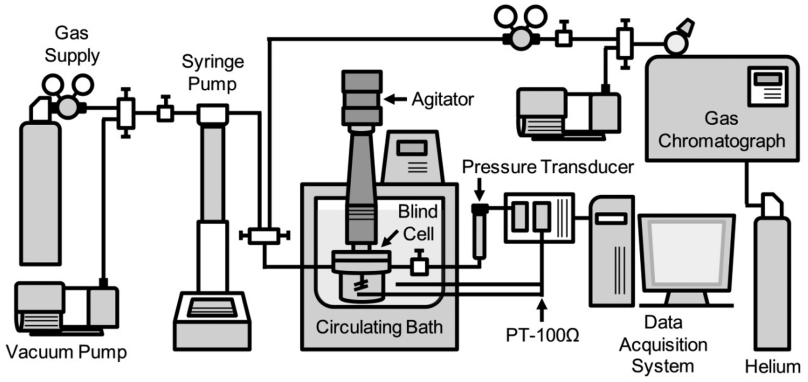

Figure 1. Schematic diagram of experimental apparatus for gas hydrate phase equilibria.

equilibrium states of single guest hydrates are characterized by one-dimensional phase boundaries in the $p-T$ diagrams. In contrast, to construct phase diagrams of binary and ternary mixed gas hydrate systems, the two-dimensional plots are accompanied by orthogonal projections of the three-dimensional spaces. Such technical considerations were recently described by Beltran et al.[32] and summarized as follows: (1) Unlike equilibrium pressure and temperature, precise control of composition in the three coexisting phases is beyond the scope of the experiment. (2) It should be noted that an initial feed composition of gas mixtures is not necessarily equivalent to an equilibrium composition. (3) The equilibrium composition of the vapor phase (y_i) is the primary intensive variable and much more accessible than hydrate phase composition (z_i) on an experimental basis. In addition, we note that the sustaining of the desired temperatures will provide an advantage in terms of the elapsed time for thermodynamic equilibrium.[33] These statements lead to the idea that experimental determinations of isotherms ($p-y_i$ diagram) can be used to understand the complicated phase equilibria of mixed gas hydrate systems.

Under isothermal operations, the equilibrium pressure and phase composition have to be specified, although only the pressure enables the formation and dissociation of hydrates. Thus, almost all instrumental techniques use an equilibrium cell equipped with sight glasses for visual observation and induce a discrete dissociation of hydrates.[10−14,33−38] Sugahara et al.[34] and Makino et al.[35] developed an experimental determination of hydrate phase composition at equilibrium by using single crystals. Makogon et al.[36,37] introduced the trial and error procedure through the spontaneously approximated pressure without a visual observation window. Nevertheless, all of the aforementioned techniques require attended operation for the dissociation process, suggesting that extensive measurements of isothermal phase equilibrium need to be performed. Still, many phase analysis studies on mixed gas hydrates have relied on modeling and simulation, which implies that their predicted results are awaiting experimental confirmation.[5,41−45]

In this work, we introduce an improved instrumental technique for determining isothermal phase equilibria of gas hydrates with multiple guests. It is shown that the equilibrium conditions of gas hydrate systems can be measured not by static but by continuous dissociation of hydrates induced by infinitesimal vapor volume expansion. During this process, the temperature of aqueous phase containing hydrates indicates the conversion of heat flow from the endothermic dissociation to external conduction. The validity of the experimental procedure for application to multiple guest systems is investigated by repeated measurements of pure gas hydrate phase equilibria. A technique that is newly developed in the present work enables unattended operation to define the dissociation pressure of gas hydrates at a constant temperature. It establishes a foundation for the further research of isothermal structural transitions dealing with the thermophysical properties of complex gas hydrate systems.

2. EXPERIMENTAL SECTION

2. 1. Materials and Apparatus. CH_4 and C_2H_6 gases were purchased from Special Gas (Korea) with stated minimum purities of 99.99 and 99.95%, respectively. Ultrahigh-purity water was obtained from a Millipore purification unit. A schematic diagram of the experimental apparatus used in this work is presented in Figure 1. The equilibrium cell was a bolted closure-type high-pressure vessel made of stainless steel. This blind cell was assembled with a vertical magnetic drive agitator. The maximum allowable operating pressure was 33 MPa, and the internal volume was 100 cm^3. A four-wire type Pt-100Ω probe was used for the temperature sensing devices with a full scale accuracy of ±0.05%. The temperature was calibrated using an ASTM 63C nitrogen-filled thermometer with 0.1 K precision. The pressure transducer (Druck, PMP5073) had an accuracy to 0.20% of full scale with a range of 0−70 MPa sealed gauge. A digital pressure gauge (Druck, DPI 104) for pressure calibration was accredited as a testing laboratory by the Korea Laboratory Accreditation Scheme (KOLAS). The total volume of the system was controlled by using a microflow syringe pump (Teledyne, ISCO 500D). The syringe pump was able to operate up to 25.86 MPa with full capacity of 507.37 mL. The syringe volume and flow rate were monitored by the pump controller display (Teledyne, ISCO D-Series). The vapor pressure in the closed system was dominated by the pump controller.

The operating temperature was maintained with a circulating bath (Jeio Tech., RW-2040G) with a stability of ±0.05 K. Two temperature sensors were placed in the bottom of the pressure vessel (internal temperature) and ethanol bath (external temperature). An analog-to-digital converter (ADC) was connected to the computer for pressure and temperature monitoring. All readings were automatically recorded using a data acquisition system with a saving interval of 1 s. The vacuum was produced by a rotary valve oil pump (Edwards, RV3). Gas from a high-pressure cylinder was fed into the syringe and vessel to a desired pressure by a gas regulator (Chiyoda Seiki, TKR-100K, 0−25 MPa).

The water-free vapor composition in equilibrium was analyzed by gas chromatograph (Young-Lin, YL 6100 GC) equipped with a thermal conductivity detector (TCD) using a Porapak N column (8 ft length × $^1/_8$ in. outer diameter). The column oven temperature was 140 °C, and the injector and detector were held at 150 °C. High-purity He (N50 quality) was used as the carrier gas at a flow rate of 30 mL/min. Sample injections were performed using a Rheodyne 7413 microscale injection valve containing a 1 μL internal loop. The loading pressure was maintained at 0.50 MPa by a line pressure regulator valve

dx.doi.org/10.1021/ef401072s | Energy Fuels 2013, 27, 5144−5152

(Chiyoda Seiki, GHN-4, 0−25 MPa). Standard gas mixtures for gas chromatograph calibration were supplied by YG Special Gas (Korea). Autochro 2000 software (Young-Lin) was utilized for data acquisition and analysis. The software was calibrated by an external standard method using two reference gas mixtures (30.07 and 70.02 mol % of CH_4 balanced with C_2H_6, respectively).

2. 2. Procedures. This section describes how to determine the equilibrium pressure of the CH_4 + H_2O system at 280 K. An amount of 10 g of liquid water was initially charged into the equilibrium cell. The mechanical agitator was assembled with the pressure vessel to hold the stirring rate at 150 rpm. The circulating bath maintained the temperature of the aqueous phase inside the blind cell at 280 K. After the vacuum operation at the maximum volume of the syringe pump (507.37 mL, exclusive of the equilibrium cell volume and dead volume), gaseous CH_4 flowed into the syringe and vessel. As shown in Figure 2, the pressure was adjusted to 4.66 MPa by the gas regulator,

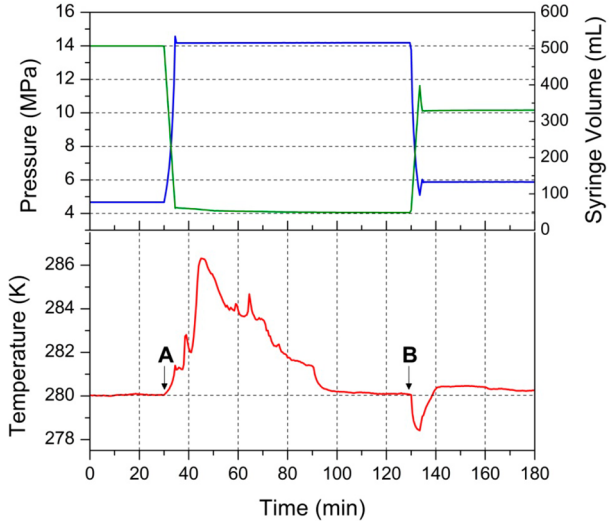

Figure 2. Plots of variation in pressure (blue), syringe volume (green), and internal temperature (red) during the formation process of CH_4 hydrates under the isothermal condition of 280 K. The operations of the syringe pump enable the formation of hydrate phase from point A and the restirring of the blind cell immediately after point B.

lower than the simply predicted dissociation pressure of CH_4 hydrates at 280 K. Then, it was pressurized to 14.17 MPa at point A and operated in constant pressure mode to induce hydrate nucleation and growth. The formation of solid hydrate crystals in the aqueous phase leads to CH_4 consumption from the gas phase, generating the corresponding exothermic heat. These two changes were detected by the pump controller display and the temperature sensor, respectively. After complete formation, the stirring of the aqueous phase was paused at 90 min. Then, heat generation did not occur, and the displacement of the syringe pump remained steady on a milliliter scale. At point B, the isobaric condition moved from 14.17 MPa to roughly 5 MPa to enable the restirring of bulk coexisting L_W−H−V phases. A temporary decrease in temperature was caused by drastic volume changes, called the "Joule−Thomson cooling effect". At the moment the agitator was restarted, the syringe pump operated in constant flow mode until the internal temperature exceeded 280 K. Then, the isobaric mode at a pressure of 5.87 MPa was operated to ensure the preservation of hydrate crystals.

Figure 3 indicates that the vapor volume expansion reduces the pressure in the blind cell. Once the syringe pump operated in refill mode with a constant flow of 150 μL/min, the endothermic dissociation reaction occurred in the aqueous phase containing solid hydrates. As this reaction proceeded, the internal temperature of the pressure vessel decreased until it reached a minimum value. Then the external heat of the circulation bath suddenly flowed into the aqueous phase beyond point C. Such a rapid recovery of temperature up to

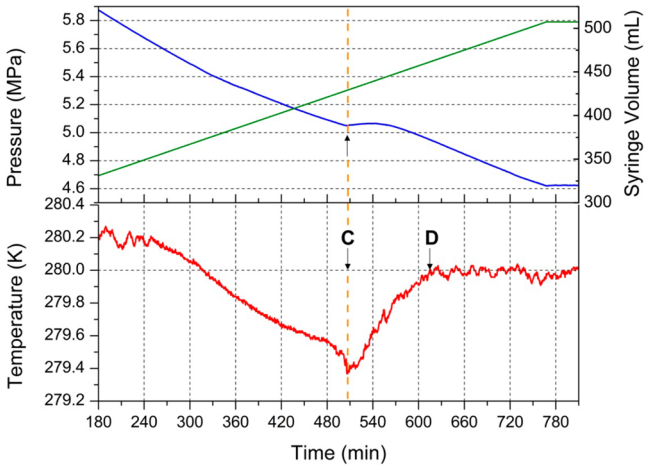

Figure 3. Plots of variation in pressure (blue), syringe volume (green), and internal temperature (red) during the dissociation process of CH_4 hydrates induced by vapor volume expansion at a rate of 150 μL/min under the isothermal condition of 280 K. The temperature profile indicates the complete dissociation of hydrate phase at point C and the recovery of the initial state at point D.

point D implies that the CH_4 hydrate decomposition no longer appears in the aqueous phase. Despite continuous operation in the refill mode of the syringe pump, the internal temperature of water-rich liquid phase in the blind cell remained unchanged. After the syringe volume reached its full capacity, the pressure and volume were restored to the initial levels. The constant operating temperature of the hydrate formation process from point A to point B may be lowered, considering the upper limit of pressure. This results from either the maximum permissible pressure in the apparatus or the vapor−liquid equilibrium (VLE) of guest mixtures. Thus, in this work, the average of the external temperature from point B to point C was defined as the isothermal condition. Then, the dissociation pressure of three coexisting phases under the corresponding isothermal condition was determined by the pressure at point C.

The equilibrium pressure of multiple gas component hydrates was defined by the identical procedure as described so far. From then on, the syringe pump operated to maintain the experimentally determined equilibrium pressure in the isobaric mode at a constant temperature. After at least an hour of stabilization in the equilibrium cell, the composition of guest mixtures was analyzed by gas chromatography. For the variation in composition of charged gas mixture, one of the gas components was flowed into the vapor phase by the pressure difference between a pure gas cylinder and system. The desired composition of the gas mixture in equilibrium was confirmed using gas chromatography.

Herein, a statistical estimation of mean values and standard deviations assessed the validity and reproducibility of repeated measurements. This statistical analysis of repeated measures was performed to determine the distribution of certain equilibrium p−T coordinates and all equilibrium vapor phase compositions of p−y_i points. Repeated data measurements of the equilibrium p−T conditions for the single gas hydrate system possessed a mean value for five coordinates exclusive of two relatively large deviation results. The mean values of y_i reported in this work were also averaged over five measured values except for the maximum and minimum compositions. Each error bar indicated the standard deviations (standard error) of the corresponding mean value. An equilibrium vapor phase composition was identified by gas chromatography with a stability of ±0.02 in mol % composition. The statistical thermodynamics program CSMGem ver. 1.10 (Colorado School of Mines, USA) predicted the phase equilibrium behavior of the gas hydrate systems. The mole fractions of water and guest gases were set at 0.30 and 0.70, respectively. The graphical presentation of the obtained

dx.doi.org/10.1021/ef401072s | Energy Fuels 2013, 27, 5144−5152

results and the analysis of fitting precision were generated using the software OriginPro 8.5 (OriginLab, USA).

2. 3. Raman Measurements. Raman spectra were collected using a dispersive Raman microscope (Horiba Jobin Yvon) equipped with a CCD detector cooled by liquid nitrogen. An Ar-ion laser with a grating of 1800 grooves/mm was used for 514.53 nm excitation. A confocal hole was set to 1000 μm, and the slit was 100 μm. The intensity of the laser was 20 mW. The sample was placed in a Linkam TMS600 cryostat cooled with liquid nitrogen during Raman scattering measurements. For all measurements, an exposure time of 5 s and an accumulation number of 5 were used. Data were collected with the software LabSpec (Horiba Jobin Yvon).

For Raman studies, sample preparation was performed under near L_W−H−V equilibrium conditions. Detailed conditions for each sample are listed in the relevant tables. After the system was vented, the pressure vessel was separated from the measuring apparatus and quenched by liquid nitrogen. Then, the solid precipitates containing hydrate crystals were directly dropped into liquid nitrogen. After the particles were ground in a mortar and pestle, the powder samples were characterized by Raman spectroscopy. Because such a process necessarily undergoes partial dissociation of hydrate phase, the samples were confirmed to be unsuitable for X-ray diffraction measurements. In this regard, we note that a previous study (Subramanian et al.[6]) provided NMR spectroscopic evidence for the Raman results.

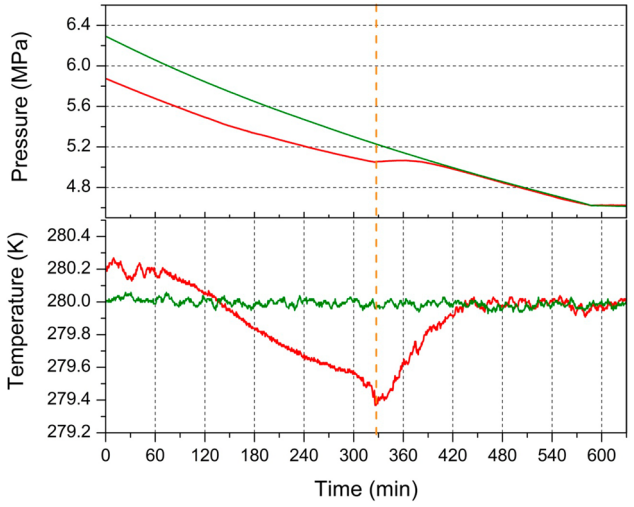

Figure 4. Comparison of pressure and temperature profiles induced by vapor volume expansion at a rate of 150 μL/min under the isothermal condition of 280 K including (red) and excluding (green) the formation process of CH_4 hydrates.

3. RESULTS AND DISCUSSION

3. 1. Automated Determination Procedure. As explained above, an infinitesimal vapor volume expansion can be used to experimentally determine endothermic hydrate dissociation points under isothermal condition. It is clearly revealed in Figure 3 that the shift from hydrate dissociation to heat conduction can be detected from internal temperature variations. At 507 min (point C), the internal temperature reached its minimum value at a temperature and pressure of 279.37 K and 5.05 MPa, respectively. The average external temperature between points B and C was 280.00 K. Accordingly, the isothermal phase equilibrium pressure of the CH_4 + H_2O system at 280.00 K was determined to be 5.05 MPa. This p−T coordinate shows a pressure difference of 0.14 MPa compared with 5.19 MPa at 280.00 K calculated by CSMGem.

In the present method, the external temperature and system volume are used as control variables during the operation of the syringe pump in refill mode. Because the pressure of the blind cell is absolutely dominated by the vapor volume expansion, the internal temperature had to be monitored to determine the equilibrium pressures of the gas hydrates. However, it was found that an inflection point of the pressure dissipation curve evidently appears at point C in Figure 3. To further understand such concurrent changes in pressure and temperature, vapor volume expansion was carried out without the formation process of hydrates. Figure 4 clearly indicates that pressure and temperature tend to rapidly recover their original levels after the minimum temperature. After this instant, as seen in the figure, the curvature of the pressure drop profile is reversed from convex to concave. Such a pressure profile supports a consistent interpretation regarding defining equilibrium at which an internal temperature indicates the minimum as a dissociation pressure under isothermal conditions.

Meanwhile, the time intervals to merge two separated profiles occur even after the decomposition of hydrates marked by a vertical line in Figure 4. It can be inferred that this phenomenon is similar to that explained previously with regard to the "memory effect" of dissociated water.[4] This suggests that an aqueous phase containing either residual crystalline phase or remaining dissolved gas has different behavior from fresh water with no previous hydrate history.[46,47] This suggests the possibility of hysteresis-like behavior of aqueous phase after gas hydrate decomposition. However, the present instrumental technique can determine hydrate phase equilibria without considering these effects because the temperature profile after the minimum is not included.

To verify the reliability of the present procedure, the existence of CH_4 hydrate phase was observed above and below the experimentally determined dissociation pressure. The overall process described earlier was carried out again at 280 K. The volume expansion rate of 150 μL/min was adapted up to about 5.20 MPa, slightly higher than 5.05 MPa (experimentally determined dissociation pressure as above). Then, the sample was quenched by liquid nitrogen at 5.14 MPa before preparation for Raman analysis (called upper sample). This procedure was repeated for the lower sample at 5.03 MPa. The quenching point for these samples is shown in Figure S1 (Supporting Information). As shown in the Raman spectra (Figure 5), for the upper sample, ν_1 symmetric C−H stretches of CH_4 in the large ($5^{12}6^2$) and small (5^{12}) cavities of structure I (sI) occur at 2904.8 and 2915.0 cm^{-1}, respectively. This indicates that the liquid nitrogen quenched sample contains typical sI CH_4 hydrates in the aqueous phase. In contrast, the Raman spectrum of the lower powder sample does not display the symmetric C−H stretch of CH_4 molecules. As expected, the hydrate phase has entirely disappeared after the pressure of the vapor phase reached the isothermal equilibrium condition. This provides evidence that the present experimental technique accurately determines the isothermal equilibrium pressure of the gas hydrate system.

3. 2. Acceptability of Instrumental Technique. To apply the proposed technique to the overall gas hydrate system, its process variables should be investigated under various conditions. First, a small volume displacement that occurred with the second pressurization after point B in Figure 2 may vary depending on the operator and the experimental conditions, thereby affecting the measuring time to some extent. Above all, the vapor volume expansion rate will play a

dx.doi.org/10.1021/ef401072s | Energy Fuels 2013, 27, 5144−5152

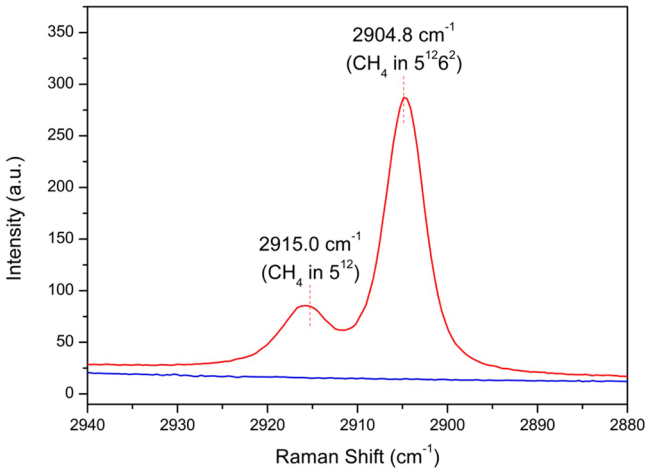

Figure 5. Raman spectra of the C−H region for CH_4 hydrates quenched from above (red) and below (blue) the experimentally determined L_W−H−V equilibrium pressure at 280 K.

crucial role in evaluating the present measurement method. According to a previous study (Tohidi et al.[48]) on the heating rate of the isochoric technique, the stepwise determination of the few but accurate equilibrium p−T conditions improves the accuracy of hydrate phase equilibria. This reflects the predictable fact that the time required to ensure thermodynamic equilibrium should be consumed in adequate amounts to reduce measurement errors. Therefore, the proposed technique also should sufficiently reduce the vapor volume expansion rate to obtain thermodynamic consistency.

Provided that the expansion rate exceeds the hydrate decomposition rate, an equilibrium pressure relatively lower than previously reported values may be experimentally determined. Such a rapid expansion rate of the syringe volume is anticipated to reduce the pressure before reaching three-phase (L_W−H−V) equilibrium under isothermal condition. Moreover, a sufficiently low rate assuring accurate measurements may be <150 μL/min. In this regard, the three-phase equilibrium of the CH_4 + H_2O system was repeatedly determined by using various rates under the isothermal condition of 280 K as listed in Table 1. As expected, this table shows that the operating variations in the expansion rate ranging from 1200 to 50 μL/min lead to an increase in dissociation pressure. We used a prespecified absolute relative deviation (ARD) from calculated values of <1% to produce reliable equilibrium conditions. Then, it is concluded that a vapor volume expansion rate up to 100 μL/min is acceptable. The repeated measurements of equilibrium p−T coordinates with vapor volume expansion at a rate of 100 μL/min in Table 1 are plotted in Figure 6. This figure shows the accuracy and stability of the present measurements comparable to predicted and previously reported equilibrium conditions.[7−11,49,50]

Table 1. Repeated Isothermal Measurements of Three-Phase (L_W−H−V) Equilibrium Pressure for Incipient CH_4 Hydrates at Various Vapor Volume Expansion Rates

rate (μL/min)	T^a (K)	p (MPa)	$p_{calcd}{}^b$ (MPa)	ARD^c (%)
1200	280.04 ± 0.008	4.70 ± 0.039	5.21	9.72
600	280.03 ± 0.003	4.93 ± 0.031	5.20	5.25
300	279.98 ± 0.008	5.12 ± 0.019	5.18	1.08
150	280.03 ± 0.006	5.13 ± 0.010	5.20	1.38
100	279.99 ± 0.009	5.18 ± 0.004	5.18	0.03
75	279.95 ± 0.003	5.18 ± 0.017	5.16	0.36
50	280.03 ± 0.009	5.25 ± 0.012	5.21	0.82

[a]Isothermal condition of 280 K. [b]Predictions of corresponding equilibrium pressure using CSMGem. [c]Absolute relative deviation (ARD) = 100 × ($|p_{calcd} - p|/p_{calcd}$).

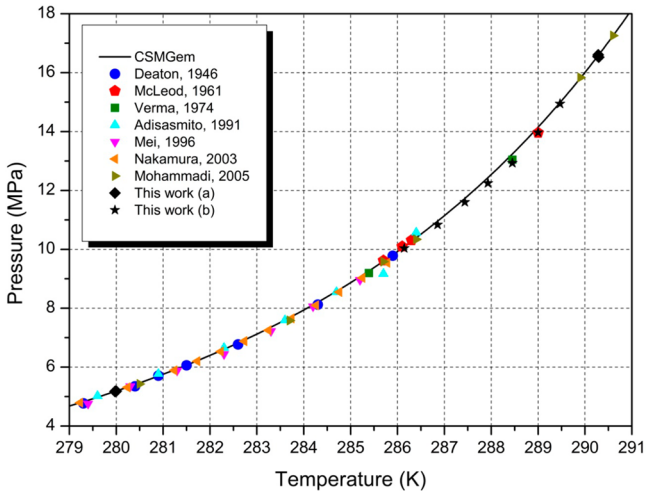

Figure 6. Three-phase (L_W−H−V) equilibrium pressure−temperature diagram for CH_4 hydrates from 279 to 291 K. (CSMGem: predicted line. Experimental data from the literature: Deaton,[7] McLeod,[8] Verma,[9] Adisasmito,[10] Mei,[11] Nakamura,[49] and Mohammadi.[50] This work: isothermal measurements with vapor volume expansion at a rate of 100 μL/min: (a) repeated measures at 280.00 and 290.30 K; (b) seven measures from 286.15 to 289.47 K.)

Even though the effect of the volume expansion rate on the equilibrium measurements was verified as above, further investigations of the reproducibility were performed at higher pressure than experimental results at 280 K. The amount of guest molecules contained in 100 μL of vapor volume changes in relation to the pressure condition. For this reason, the isothermal condition of repeated measurements was increased from 280.00 to 290.30 K. As listed in Table 2, the ARD values determined by repeated measurements under the isothermal condition of 290.30 K are still reliable for the expansion rates of 100 and 50 μL/min. Also, these two expansion rates require measuring times of about 473 and 833 min, respectively. As shown in Figure 6, these equilibrium p−T conditions determined by a vapor expansion rate of 100 μL/min were plotted in the phase diagram. In addition to 290.30 K, the adjacent equilibrium points were measured one time each in the lower temperature range at an expansion rate of 100 μL/min as listed in Table S1 (Supporting Information). Also, Figure S2 (Supporting Information) shows that the pressure and temperature profiles of the isothermal measurements at 286.15 K, respectively, reveal the inflection and minimum point as described in the previous section. All of the results so far indicate that the proposed instrumental technique based on vapor volume expansion is acceptable to determine the dissociation pressure of gas hydrates at a constant temperature. We will from now on use the expansion rate of 100 μL/min and extend the scope of the hydrate system studied with mixed gas hydrates.

3. 3. Equilibrium Isotherm Analysis. Much of the recent research on the structural behavior of CH_4 + C_2H_6 hydrates has

dx.doi.org/10.1021/ef401072s | Energy Fuels 2013, 27, 5144−5152

Table 2. Repeated Isothermal Measurements of Three-Phase (L_W−H−V) Equilibrium Pressure for Incipient CH_4 Hydrates and Measuring Time at Various Vapor Volume Expansion Rates

rate (μL/min)	T^a (K)	p (MPa)	p_{calcd} (MPa)	ARD (%)	t^b (min)
100	290.28 ± 0.005	16.56 ± 0.025	16.59	0.15	473 ± 15
50	290.29 ± 0.008	16.64 ± 0.028	16.59	0.03	833 ± 129

[a]Isothermal condition of 290.30 K. [b]Measuring time (t) = total time from the first pressurization to the recovery of the initial state (e.g., from point A in Figure 2 to point D in Figure 3).

focused on forming sII hydrates at certain composition ranges, even if this system consists of two sI formers.[6,51−59] This binary mixture system retains the structural interconversion phenomenon between sI and sII with the lower and upper transitions, respectively, for relatively methane-rich guest mixtures and dilute ethane in methane. These observations have been possible by combining phase equilibrium measurements with the existing prediction method and spectroscopic analysis. Although for the past decade such peculiar transitions have been steadily investigated since the discovery of interconversion behavior,[42,53−59] there is a need for improvement from the following viewpoints: (1) There is a lack of equilibrium p−T conditions reported, which are the most primary experimental results for analyzing isothermal phase equilibria.[40,41,56] (2) Even in isotherm analysis, consistency between spectroscopic measurements and modeling studies is not yet ensured.[6] (3) The calculated temperature dependence of the lower transitions presented as T-y_i diagrams also shows quite a different tendency from the experimentally reported behavior (particularly at 283.10 K).[41,42,59]

Therefore, the present study consolidates the foundation to resolve these problems. Above all, the instrumental technique in this work allows the extensive measurement of isothermal phase equilibrium p−y_i points owing to convenient availability and ease of handling. Apart from the extremely upper transition, the three-phase (L_W−H−V) equilibrium boundaries in the p−y_i diagrams of incipient CH_4 + C_2H_6 hydrates are distinct in the two regimes as already predicted in previous works.[5,56] To establish these equilibrium curves experimentally, a series of equilibrium p−y_i conditions was plotted on the phase diagram at constant temperature. Then, two distinct curves were obtained by nonlinear fitting of these points, and their intersection was determined as the lower transition point on the corresponding isotherm. The procedure described so far was performed at 283.10 K as follows.

First, isothermal phase equilibrium measurement of incipient CH_4 (1) + C_2H_6 (2) hydrates was carried out at 283.10 K. Table S2 (Supporting Information) lists these p−y_1 conditions in equilibrium by using volume expansion at a rate of 100 μL/min. These results are plotted in Figure 7 and crowded in a narrow range in y_1 from 0.70 to 0.78 due to evidence of cusp formation. Figure 7 indicates that the present technique produces the structural transition point close to the predictions of CSMGem. In addition, we were able to obtain a more obviously distinct curve and a more sharply defined cusp than previously reported results[59] and CSMGem, respectively. Then, to estimate the equations of the experimentally determined p−y_1 diagrams, nonlinear fitting was performed, and its results are listed in Table S3 (Supporting Information). Two fitting equations for p as a function of y_1 are found to intersect at a point where the equilibrium mole fraction of CH_4 in the vapor is 0.7358 at 2.99 MPa. This intersection point is adjacent to the actual measurements of the range in y_1 from 0.7345 to 0.7373

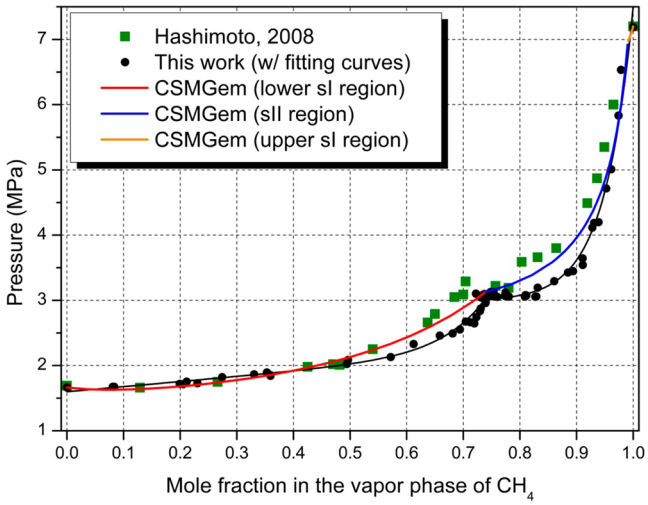

Figure 7. Isothermal three-phase (L_W−H−V) equilibrium pressure−composition (p−y_1) diagram for incipient CH_4 (1) + C_2H_6 (2) hydrates at 283.10 K (y_1 = equilibrium vapor phase mole fraction of CH_4). (Hashimoto: Experimental data from the literature.[59] This work with nonlinear fitting curve: experimental determination with vapor volume expansion at a rate of 100 μL/min. CSMGem: predictions of distinct phase boundaries with respect to the interconversion of sI and sII.)

and in the dissociation pressure from 3.04 to 3.10 as seen in Table S2 (Supporting Information).

Even if we have relatively easily identified the lower transition points by using only experimental measurements, the Raman spectra were used for the reliable confirmation of the structural transitions of CH_4 + C_2H_6 hydrates. Four different powder samples were prepared near the equilibrium pressure of each CH_4 (1) + C_2H_6 (2) hydrate for Raman analysis as listed in Table 3. Note that there is a need for a significant period of time (more than a day) to ensure the intrinsic crystal structure due to the metastable region near the lower transition point.[52−55] The overall analysis procedure followed the method described in more detail by Subramanian et al.[6] but narrowed the experimentally determined range in y_1 from about 0.63−

Table 3. Isothermal Measurements of Three-Phase (L_W−H−V) Equilibrium Pressure for Incipient CH_4 (1) + C_2H_6 (2) Hydrates Prepared for Raman Analysis

y_1	T^a (K)	p^b (MPa)	$p_{qcd}{}^c$ (MPa)	$(p_{qcd} - p)/p \times 100$ (%)	no. of Raman spectra
0.7307	283.10	2.87	2.92	1.70	7
0.7394	283.09	2.97	3.02	1.89	10
0.7481	283.11	3.13	3.18	1.54	9
0.7534	283.08	3.12	3.18	1.91	7

[a]Isothermal condition of 283.10 K. [b]Experimental determination with vapor volume expansion at a rate of 100 μL/min. [c]Pressure at which sample was preserved and quenched.

dx.doi.org/10.1021/ef401072s | Energy Fuels 2013, 27, 5144−5152

0.92 to 0.73−0.75. Figure 8 shows that the ν_3 C−C stretches of C_2H_6 occur at frequencies of 1000.9 and 992.9 cm^{-1},

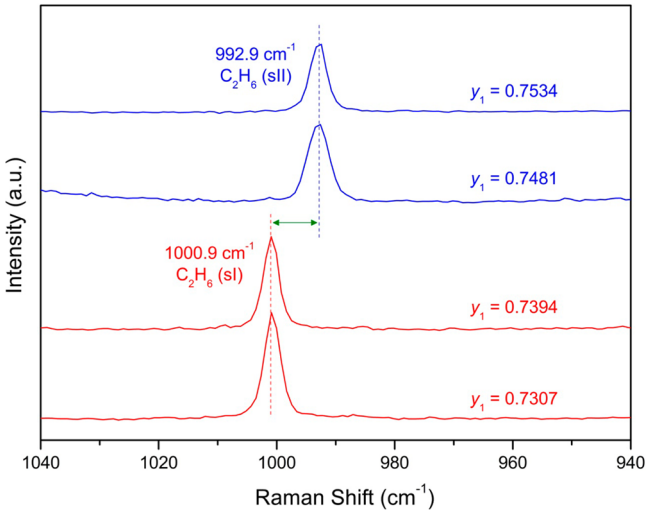

Figure 8. Raman spectra of the C−C stretching vibration of C_2H_6 for incipient CH_4 (1) + C_2H_6 (2) hydrates quenched close to L_W−H−V equilibrium pressure at 283.10 K (y_1 = equilibrium vapor phase mole fraction of CH_4).

respectively, corresponding to large cavities in sI ($5^{12}6^2$) and sII ($5^{12}6^4$) as previously reported.[6,59] These spectra evidently reflect the lower transition with y_1 in the range from 0.7394 to 0.7481, respectively, from sI to sII. Figure 9 illustrates the

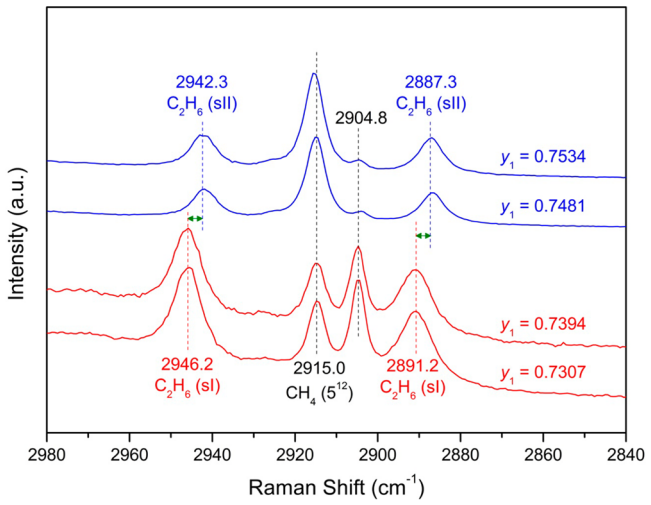

Figure 9. Raman spectra of the C−H region for incipient CH_4 (1) + C_2H_6 (2) hydrates quenched close to L_W−H−V equilibrium pressure at 283.10 K (y_1 = equilibrium vapor phase mole fraction of CH_4).

resonance doublet Raman bands of C_2H_6 in the C−H region being expected to obtain two strong peaks. Two frequencies at 2891.2 and 2946.2 cm^{-1} correspond to C_2H_6 in sI hydrate large ($5^{12}6^2$) cavities, whereas the Raman bands at 2887.3 and 2942.3 cm^{-1} were assigned to sII hydrate large ($5^{12}6^4$) cavities. In addition to C_2H_6, Figure 9 indicates that the relative intensity inversion of the two ν_1 C−H stretches of CH_4 can be attributed to the structural transition between sI and sII.

As presently determined by Raman studies, the lower transition composition shows the range in y_1 from 0.7394 to 0.7481, which is comparable to results of isothermal phase equilibrium measurements in the present work. All of the outcomes estimated by different methods for the lower transition point defined at 283.10 K are summarized in Table 4. Two predicted y_1 values of about 0.74 (Ballard et al.[41]) and

Table 4. Summary of Studies on Conditions of Pressure−Composition of Isothermal Structural Transitions in Incipient CH_4 (1) + C_2H_6 (2) Gas Hydrates for Lower Transition Point (from sI to sII) at 283.10 K

operator	p (MPa)	y_1	type of procedure applied
Hashimoto[59]	3.01	0.68	mass and volume balance calculation
this work[a]	3.1293	0.7389	Gibbs energy minimization model
this work[b]	3.0384−3.0960	0.7345−0.7373	phase equilibrium measurements
this work	2.9688−3.1282	0.7394−0.7481	Raman spectroscopic analysis

[a]Predictions using CSMGem. [b]Experimental determination with vapor volume expansion at a rate of 100 μL/min.

0.82 (Klauda et al.[42]) are not included in this table because these calculations were presented not as values but as diagrams. Table 4 shows that two entirely experimental determinations of the lower transition point in this work closely correspond to each other; moreover, these are nearly identical to the predicted results, at least under the isothermal condition of 283.10 K. This raises the exciting possibility that additional experimental observations could easily construct the entire boundary of sII hydrates in T−y_1 diagrams for the CH_4 (1) + C_2H_6 (2) + H_2O system.[41,42]

4. CONCLUSIONS

Controlling an extensive variable, the closed system volume, provides a major contribution to the development of the instrumental technique as described so far. Although vapor volume expansion has been applied to the isothermal measurement of gas hydrate phase equilibrium, it has been limited to the stepwise dissociation of hydrate phase.[11,38−40] The reliability of the proposed method was validated by the inflection point of the pressure dissipation curve and the Raman spectra for quenched samples. As a test of the acceptability of the present method, repeated measurement of isothermal phase equilibrium was carried out using pure CH_4 hydrate, thereby determining the optimal operation rate to be 100 μL/min. This new method can offer advantages and improvements in measuring hydrate phase equilibria with multiple guests. In addition, it can be applied not only to binary gas hydrates but also to ternary guest hydrates requiring more extensive measurement and sophisticated analysis.[5]

The scope of this technique was extended to the structural analysis of CH_4 + C_2H_6 hydrates. The intrinsic crystal structure of gas hydrate systems has been extensively investigated with respect to the molecular size of guest species. Also, the structure of mixed gas hydrates and their coexistence are strongly dependent on the preference of guest mixtures for certain types of water clusters and the large to small cavity ratio in the unit cell.[57] These investigations on the intrinsic properties of hydrate systems have consistently performed

dx.doi.org/10.1021/ef401072s | Energy Fuels 2013, 27, 5144−5152

from fundamental and practical aspects, which is still challenging with currently available techniques.[1,3] In particular, variations in the equilibrium phase composition of $CH_4 + C_2H_6$ hydrates have serious implications for the thermophysical properties of NGH.[6,41] The guest component of NGH mainly consists of CH_4 with a small amount of C_2H_6 and C_3H_8, although the precise composition differs on the basis of various origins of CH_4 in the earth.[18,19] The results of studies on the intrinsic properties of $CH_4 + C_2H_6$ hydrates are applicable to the prediction of thermophysical parameters of NGH with mass and energy balance calculations.[41,52]

In this work, the isotherm analysis of $CH_4 + C_2H_6$ hydrates further focuses on the abnormal behavior of the lower transition point at which the structural transitions occur with a change of concavity.[41,42] These reflect the fact that the temperature affects the preferential partitioning of gas molecules into several cavities, thereby shifting the structural transition point on each isotherm. The first step of this approach was to determine the lower transition point of incipient $CH_4 + C_2H_6$ hydrates at 283.10 K. As expected, the extensive equilibrium $p-y_i$ coordinates on the isotherm enable the entirely experimental approach of determining the structural transition behavior comparable to Raman spectra and CSMGem. The results of further studies will demonstrate that the temperature-dependent enclathration of gaseous species provides understanding of the intrinsic properties of mixed gas hydrates. Even though a few binary mixed gas hydrates are verified or expected not to undergo such structural transformations, these experimental findings will develop new insights into the selective encaging behavior of various guest molecules.

■ ASSOCIATED CONTENT

Supporting Information

Pressure−volume diagrams of the quenching point of upper and lower samples prepared for Raman analysis; plots of variation in pressure and internal temperature during the dissociation process of CH_4 hydrates induced by vapor volume expansion at a rate of 100 μL/min; isothermal measurements of L_W-H-V equilibrium for incipient CH_4 and $CH_4 + C_2H_6$ hydrates with vapor volume expansion at a rate of 100 μL/min. This material is available free of charge via the Internet at http://pubs.acs.org.

■ AUTHOR INFORMATION

Corresponding Author

*(H.L.) Phone: +82-42-350-3917. Fax: +82-42-350-3910. E-mail: h_lee@kaist.ac.kr.

Notes

The authors declare no competing financial interest.

■ ACKNOWLEDGMENTS

This research was funded by the National Research Foundation of Korea (NRF) (No. 2010-0029176) and by the WCU program (No. 31-2008-000-10055-0) through a grant from the Ministry of Science, ICT, and Future Planning (MSIP). This research was also supported by the MSIP through the "Recovery of Natural Methane Gas Hydrate from Injection of Carbon Dioxide and Nitrogen" project of Korea Institute of Geoscience and Mineral Resources (KIGAM) and Gas Hydrate R&D Organization.

■ REFERENCES

(1) Sloan, E. D. Fundamental principles and applications of natural gas hydrates. *Nature (London, U.K.)* **2003**, *426*, 353−359.
(2) Sloan, E. D. Gas hydrates: review of physical/chemical properties. *Energy Fuels* **1998**, *12* (2), 191−196.
(3) Ripmeester, J. A. Hydrate research-from correlations to a knowledge-based discipline: the importance of structure. *Ann. N.Y. Acad. Sci.* **2000**, *912* (1), 1−16.
(4) Sloan, E. D.; Koh, C. A. *Clathrate Hydrates of Natural Gases*, 3rd ed.; CRC Press (Taylor and Francis Group): Boca Raton, FL, 2008.
(5) Ballard, A. L.; Sloan, E. D. Hydrate phase diagrams for methane + ethane + propane mixtures. *Chem. Eng. Sci.* **2001**, *56* (24), 6883−6895.
(6) Subramanian, S.; Kini, R. A.; Dec, S. F.; Sloan, E. D. Evidence of structure II hydrate formation from methane+ethane mixtures. *Chem. Eng. Sci.* **2000**, *55* (11), 1981−1999.
(7) Deaton, W. M.; Frost, E. M. Clathrate hydrates and their relation to the operations of natural gas pipelines. *U.S. Bureau of Mines Monograph* **1946**, *No. 8*.
(8) McLeod, H. O.; Campbell, J. M. Natural gas hydrates at pressures to 10,000 psia. *J. Petrol. Technol.* **1961**, *222*, 590.
(9) Verma, V. K.; Hand, J. H.; Katz, D. L. *Gas Hydrates from Liquid Hydrocarbons (Methane-Propane-Water System)*; GVC/AIChE Joint Meeting, Munich, Germany, 1974; p 10.
(10) Adisasmito, S.; Frank, R. J.; Sloan, E. D. Hydrates of carbon dioxide and methane mixtures. *J. Chem. Eng. Data* **1991**, *36* (1), 68−71.
(11) Mei, D.-H.; Liao, J.; Yang, J.-T.; Guo, T.-M. Experimental and modeling studies on the hydrate formation of a methane + nitrogen gas mixture in the presence of aqueous electrolyte solutions. *Ind. Eng. Chem. Res.* **1996**, *35* (11), 4342−4347.
(12) Otto, F. D.; Robinson, D. B. A study of hydrates in the methane-propylene-water system. *AIChE J.* **1960**, *6* (4), 602−605.
(13) Jhaveri, J.; Robinson, D. B. Hydrates in the methane-nitrogen system. *Can. J. Chem.* **1965**, *43* (2), 75−78.
(14) Holder, G. D.; Hand, J. H. Multiple-phase equilibria in hydrates from methane, ethane, propane and water mixtures. *AIChE J.* **1982**, *28* (3), 440−447.
(15) Nixdorf, J.; Oellrich, L. R. Experimental determination of hydrate equilibrium conditions for pure gases, binary and ternary mixtures and natural gases. *Fluid Phase Equilib.* **1997**, *139* (1−2), 325−333.
(16) Sloan, E. D.; Koh, C. A.; Sum, A. K. *Natural Gas Hydrates in Flow Assurance*; Elsevier: Amsterdam, The Netherlands, 2010.
(17) Panter, J. L.; Ballard, A. L.; Sum, A. K.; Sloan, E. D.; Koh, C. A. Hydrate plug dissociation via nitrogen purge: experiments and modeling. *Energy Fuels* **2011**, *25* (6), 2572−2578.
(18) Hester, K. C.; Dunk, R. M.; Walz, P. M.; Peltzer, E. T.; Sloan, E. D.; Brewer, P. G. Direct measurements of multi-component hydrates on the seafloor: pathways to growth. *Fluid Phase Equilib.* **2007**, *261* (1−2), 396−406.
(19) Hester, K. C.; Brewer, P. G. Clathrate hydrates in nature. *Annu. Rev. Mar. Sci.* **2009**, *1* (1), 303−327.
(20) Khokhar, A. A.; Gudmundsson, J. S.; Sloan, E. D. Gas storage in structure H hydrates. *Fluid Phase Equilib.* **1998**, *150−151*, 383−392.
(21) Cha, I.; Lee, S.; Lee, J. D.; Lee, G.-w.; Seo, Y. Separation of SF_6 from gas mixtures using gas hydrate formation. *Environ. Sci. Technol.* **2010**, *44* (16), 6117−6122.
(22) Lee, H.-H.; Ahn, S.-H.; Nam, B.-U.; Kim, B.-S.; Lee, G.-W.; Moon, D.; Shin, H. J.; Han, K. W.; Yoon, J.-H. Thermodynamic stability, spectroscopic identification, and gas storage capacity of $CO_2-CH_4-N_2$ mixture gas hydrates: implications for landfill gas hydrates. *Environ. Sci. Technol.* **2012**, *46* (7), 4184−4190.
(23) Kang, S.-P.; Lee, H. Recovery of CO_2 from flue gas using gas hydrate: thermodynamic verification through phase equilibrium measurements. *Environ. Sci. Technol.* **2000**, *34* (20), 4397−4400.
(24) Linga, P.; Adeyemo, A.; Englezos, P. Medium-pressure clathrate hydrate/membrane hybrid process for postcombustion capture of carbon dioxide. *Environ. Sci. Technol.* **2007**, *42* (1), 315−320.

(25) Ohgaki, K.; Takano, K.; Sangawa, H.; Matsubara, T.; Nakano, S. Methane exploitation by carbon dioxide from gas hydrates: phase equilibria for CO_2-CH_4 mixed hydrate system. *J. Chem. Eng. Jpn.* **1996**, *29* (3), 478−483.
(26) Lee, H.; Seo, Y.; Seo, Y.-T.; Moudrakovski, I. L.; Ripmeester, J. A. Recovering methane from solid methane hydrate with carbon dioxide. *Angew. Chem., Int. Ed.* **2003**, *42* (41), 5048−5051.
(27) Park, Y.; Kim, D.-Y.; Lee, J.-W.; Huh, D.-G.; Park, K.-P.; Lee, J.; Lee, H. Sequestering carbon dioxide into complex structures of naturally occurring gas hydrates. *Proc. Natl. Acad. Sci. U.S.A.* **2006**, *103* (34), 12690−12694.
(28) Ota, M.; Saito, T.; Aida, T.; Watanabe, M.; Sato, Y.; Smith, R. L.; Inomata, H. Macro and microscopic CH_4−CO_2 replacement in CH_4 hydrate under pressurized CO_2. *AIChE J.* **2007**, *53* (10), 2715−2721.
(29) Shin, K.; Park, Y.; Cha, M.; Park, K.-P.; Huh, D.-G.; Lee, J.; Kim, S.-J.; Lee, H. Swapping phenomena occurring in deep-sea gas hydrates. *Energy Fuels* **2008**, *22* (5), 3160−3163.
(30) Koh, D.-Y.; Kang, H.; Kim, D.-O.; Park, J.; Cha, M.; Lee, H. Recovery of methane from gas hydrates intercalated within natural sediments using CO_2 and a CO_2/N_2 gas mixture. *ChemSusChem* **2012**, *5* (8), 1443−1448.
(31) Gupta, A. K.; Raj Bishnoi, P.; Kalogerakis, N. A method for the simultaneous phase equilibria and stability calculations for multiphase reacting and non-reacting systems. *Fluid Phase Equilib.* **1991**, *63* (1−2), 65−89.
(32) Beltran, J. G.; Bruusgaard, H.; Servio, P. Gas hydrate phase equilibria measurement techniques and phase rule considerations. *J. Chem. Thermodyn.* **2012**, *44* (1), 1−4.
(33) Hütz, U.; Englezos, P. Measurement of structure H hydrate phase equilibrium and the effect of electrolytes. *Fluid Phase Equilib.* **1996**, *117* (1−2), 178−185.
(34) Sugahara, T.; Makino, T.; Ohgaki, K. Isothermal phase equilibria for the methane + ethylene mixed gas hydrate system. *Fluid Phase Equilib.* **2003**, *206* (1−2), 117−126.
(35) Makino, T.; Tongu, M.; Sugahara, T.; Ohgaki, K. Hydrate structural transition depending on the composition of methane + cyclopropane mixed gas hydrate. *Fluid Phase Equilib.* **2005**, *233* (2), 129−133.
(36) Makogon, T. Y.; Sloan, E. D. Phase equilibrium for methane hydrate from 190 to 262 K. *J. Chem. Eng. Data* **1994**, *39* (2), 351−353.
(37) Makogon, T. Y.; Mehta, A. P.; Sloan, E. D. Structure H and structure I hydrate equilibrium data for 2,2-dimethylbutane with methane and xenon. *J. Chem. Eng. Data* **1996**, *41* (2), 315−318.
(38) Englezos, P.; Bishnoi, P. R. Experimental study on the equilibrium ethane hydrate formation conditions in aqueous electrolyte solutions. *Ind. Eng. Chem. Res.* **1991**, *30* (7), 1655−1659.
(39) Bruusgaard, H.; Beltrán, J. G.; Servio, P. Vapor−liquid water−hydrate equilibrium data for the system N_2 + CO_2 + H_2O. *J. Chem. Eng. Data* **2008**, *53* (11), 2594−2597.
(40) Bruusgaard, H.; Carbone, A.; Servio, P. H−L_W−V equilibrium measurements for the CH_4 + C_2H_6 + H_2O hydrate forming system. *J. Chem. Eng. Data* **2010**, *55* (9), 3680−3683.
(41) Ballard, A. L.; Sloan, E. D. Optimizing thermodynamic parameters to match methane and ethane structural transition in natural gas hydrate equilibria. *Ann. N.Y. Acad. Sci.* **2000**, *912* (1), 702−712.
(42) Klauda, J. B.; Sandler, S. I. Phase behavior of clathrate hydrates: a model for single and multiple gas component hydrates. *Chem. Eng. Sci.* **2003**, *58* (1), 27−41.
(43) Anderson, B. J.; Bazant, M. Z.; Tester, J. W.; Trout, B. L. Application of the cell potential method to predict phase equilibria of multicomponent gas hydrate systems. *J. Phys. Chem. B* **2005**, *109* (16), 8153−8163.
(44) Herri, J. M.; Bouchemoua, A.; Kwaterski, M.; Fezoua, A.; Ouabbas, Y.; Cameirao, A. Gas hydrate equilibria for CO_2−N_2 and CO_2−CH_4 gas mixtures − experimental studies and thermodynamic modelling. *Fluid Phase Equilib.* **2011**, *301* (2), 171−190.
(45) Moradi, G.; Khosravani, E. Modeling of hydrate formation conditions for CH_4, C_2H_6, C_3H_8, N_2, CO_2 and their mixtures using the PRSV2 equation of state and obtaining the Kihara potential parameters for these components. *Fluid Phase Equilib.* **2013**, *338*, 179−187.
(46) Makogon, Y. F. *Hydrates of Natural Gas*; Moscow, Nedra, Izadatelstro (1974 in Russian) Transl. J. Cieslesicz; PennWell Books: Tulsa, OK, 1981; p 237.
(47) Rodger, P. M. Methane hydrate: melting and memory. *Ann. N.Y. Acad. Sci.* **2000**, *912* (1), 474−482.
(48) Tohidi, B.; Burgass, R. W.; Danesh, A.; Østergaard, K. K.; Todd, A. C. Improving the accuracy of gas hydrate dissociation point measurements. *Ann. N.Y. Acad. Sci.* **2000**, *912* (1), 924−931.
(49) Nakamura, T.; Makino, T.; Sugahara, T.; Ohgaki, K. Stability boundaries of gas hydrates helped by methane-structure-H hydrates of methylcyclohexane and cis-1,2-dimethylcyclohexane. *Chem. Eng. Sci.* **2003**, *58* (2), 269−273.
(50) Mohammadi, A. H.; Anderson, R.; Tohidi, B. Carbon monoxide clathrate hydrates: equilibrium data and thermodynamic modeling. *AIChE J.* **2005**, *51* (10), 2825−2833.
(51) Hester, K. C.; Sloan, E. D. sII structural transitions from binary mixtures of simple sI formers. *Int. J. Thermophys.* **2005**, *26* (1), 95−106.
(52) Subramanian, S.; Ballard, A. L.; Kini, R. A.; Dec, S. F.; Sloan, E. D. Structural transitions in methane + ethane gas hydrates − part I: upper transition point and applications. *Chem. Eng. Sci.* **2000**, *55* (23), 5763−5771.
(53) Takeya, S.; Kamata, Y.; Uchida, T.; Nagao, J.; Ebinuma, T.; Narita, H.; Hori, A.; Hondoh, T. Coexistence of structure I and II hydrates formed from a mixture of methane and ethane gases. *Can. J. Phys.* **2003**, *81* (1−2), 479−484.
(54) Kida, M.; Jin, Y.; Takahashi, N.; Nagao, J.; Narita, H. Dissociation behavior of methane−ethane mixed gas hydrate coexisting structures I and II. *J. Phys. Chem. A* **2010**, *114* (35), 9456−9461.
(55) Ohno, H.; Strobel, T. A.; Dec, S. F.; Sloan, E. D.; Koh, C. A. Raman studies of methane−ethane hydrate metastability. *J. Phys. Chem. A* **2009**, *113* (9), 1711−1716.
(56) Ballard, A. L.; Sloan, E. D. Structural transitions in methane + ethane gas hydrates − part II: modeling beyond incipient conditions. *Chem. Eng. Sci.* **2000**, *55* (23), 5773−5782.
(57) Uchida, T.; Takeya, S.; Kamata, Y.; Ikeda, I. Y.; Nagao, J.; Ebinuma, T.; Narita, H.; Zatsepina, O.; Buffett, B. A. Spectroscopic observations and thermodynamic calculations on clathrate hydrates of mixed gas containing methane and ethane: determination of structure, composition and cage occupancy. *J. Phys. Chem. B* **2002**, *106* (48), 12426−12431.
(58) Kawamura, T.; Ohga, K.; Higuchi, K.; Yoon, J. H.; Yamamoto, Y.; Komai, T.; Haneda, H. Dissociation behavior of pellet-shaped methane−ethane mixed gas hydrate samples. *Energy Fuels* **2003**, *17* (3), 614−618.
(59) Hashimoto, S.; Sasatani, A.; Matsui, Y.; Sugahara, T.; Ohgaki, K. Isothermal phase equilibria for methane + ethane + water ternary system containing gas hydrates. *Open Thermodyn. J.* **2008**, *2*, 100−105.